Inorg. Chem. **2008**, *47*, 1067–1073

A Distorted Cubic Tetranuclear Copper(II) Phosphonate Cage with a Double-Four-Ring-Type Core

Vadapalli Chandrasekhar,*,† Loganathan Nagarajan,† Rodolphe Clérac,‡ Surajit Ghosh,† and Sandeep Verma†

Department of Chemistry, Indian Institute of Technology—Kanpur, Kanpur-208 016, India, and Centre de Recherche Paul Pascal, CNRS, UPR8641, Université Bordeaux 1, 115 avenue du Dr. A. Schweitzer, 33600 Pessac, France

Received October 2, 2007

The reaction of $Cu_2(O_2CMe)_4 \cdot 2H_2O$ with *tert*-butylphosphonic acid and 3,5-di-*tert*-butylpyrazole in the presence of triethylamine leads to a high-yield synthesis of the tetranuclear compound $[Cu_2(3,5\text{-}t\text{-}Bu_2PzH)_2(t\text{-}BuPO_3)_2]_2$ (**1**). The latter has a distorted cubic cage structure and its core resembles the D4R (double-four-ring) motif found in zeolites. The phosphonate, $[t\text{-}BuPO_3]^{2-}$, functions as a dianionic tridentate ligand, while the pyrazole ligands are neutral and are monodentate. The coordination geometry at each copper atom is distorted square planar with a 3O,1N coordination environment. Magnetic measurements on **1** reveal that the χT product continuously decreases to reach a value very close to zero at 1.8 K, indicating dominant antiferromagnetic interactions between Cu(II) ions that leads to an $S = 0$ ground state. The tetranuclear cage **1** functions as a very effective artificial nuclease in the presence of an external oxidant, magnesium monoperoxyphthalate.

Introduction

One-, two-, and three-dimensional transition metal phosphonates have been very well studied.[1] These possess extended structures, and many of them have potential applications in various fields such as cation exchangers,[2] ion-sensors,[3] NLO materials,[4] medical diagonosis,[5] or even as supports for preparing oligonucleotide arrays.[6] In contrast to these well-researched systems, zero-dimensional or molecular metal phosphonates have only begun to attract attention in recent years.[7] However, there is already sufficient data to indicate that the multiple coordination modes provided by the phosphonate ligand enable it to mediate the assembly of multimetallic architectures possessing diverse structures. One of the synthetic difficulties in the assembly of these compounds is to overcome the insolubility of transition metal phosphonates. This can be achieved by a combination of strategies, including the use of a sterically hindered phosphonic acid.[8] The additional use of an ancillary ligand not only provides structural stability to the metal phosphonate but often induces lipophilicity. Using this approach, we and others have prepared different types of discrete transition metal phosphonates.[8a,9] In addition to possessing interesting structures, some of these soluble assemblies have novel magnetic[10] or optical properties.[11]

* To whom correspondence should be addressed. Fax: 91-512-2590007/2597436; Tel: 91-512-2597259; E-mail: vc@iitk.ac.in.
† Indian Institute of Technology—Kanpur.
‡ Université Bordeaux 1.

(1) (a) Alberti, G.; Costantino, U.; Allulli, S.; Tomassini, N. *J. Inorg. Nucl. Chem.* **1978**, *40*, 1113. (a) Clearfield, A. *Prog. Inorg. Chem.* **1998**, *47*, 371. (b) Cao, G.; Hong, H. G.; Mallouk, T. E. *Acc. Chem. Res.* **1992**, *25*, 420. (c) Thompson, M. E. *Chem. Mater.* **1994**, *6*, 1168. (d) Du, Z.-Y.; Xu H.-B.; Mao, J.-G. *Inorg. Chem.* **2006**, *45*, 9780 and references therein.
(2) (a) Alberti, G. *Acc. Chem. Res.* **1978**, *11*, 163. (b) Jaber, M.; Larlus, O.; Mieche-Brendle, J. *Solid State Sci.* **2007**, *9*, 144.
(3) Alberti, G.; Casciola, M.; Polombari, R. *Solid State Ionics* **1992**, *52*, 291.
(4) (a) Katz, H. E.; Schiller, G.; Putvinski, T. M.; Schilling, M. L.; Wilson, W. L.; Chidsey, C. E. D. *Science* **1991**, *254*, 1485. (b) Ayyapan, P.; Evans, O. R.; Cui, Y.; Wheeler, K. A.; Lin, W. *Inorg. Chem.* **2002**, *41*, 4978.
(5) Mondry A.; Janicki, R. *Dalton Trans.* **2006**, 4702 and references therein.
(6) Bujoli, B.; Lane, S. M.; Nonglaton, G.; Pipelier, M.; Léger, J.; Talham D. R.; Tellier, C. *Chem. Eur. J.* **2005**, *11*, 1980 references therein.
(7) (a) Walawalkar, M. G.; Roesky, H. W.; Murugavel, R. *Acc. Chem. Res.* **1999**, *32*, 117. (b) Burkholder, E.; Goulub, V.; O'Conner, C. J.; Zubieta, J. *Chem. Commun.* **2003**, 2128. (c) Cador, O.; Gatteschi, D.; Sessoli, R.; Larson, F. K.; Overgaard, J.; Barra, A.-L.; Teat, S. J.; Timco, G. A.; Winpenny, R. E. P. *Angew. Chem., Int. Ed.* **2004**, *43*, 5196. (d) Du, Z-Y.; Bu, H-B.; Mao, J-G. *Inorg. Chem.* **2006**, *45*, 6424.
(8) (a) Chandrasekhar, V.; Sasikumar, P.; Boomishankar R.; Anantharaman, G. *Inorg. Chem.* **2006**, *45*, 3344 references therein. (b) Baskar, V.; Shanmugam, M.; Saňudo, E. C.; Shanmugam, M.; Collison, D.; McInnes, E. J. L.; Wei Q.; Winpenny, R. E. P. *Chem. Commun.* **2007**, 37. (c) Konar, S.; Bhuvanesh, N.; Clearfield, A. *J. Am. Chem. Soc.* **2006**, *128*, 9604. (d) Taylor, J. M.; Mahmoudkhani A. H.; Shimizu, G. K. H. *Angew. Chem., Int. Ed.* **2007**, *46*, 795 references therein.

10.1021/ic701948g CCC: $40.75
Published on Web 01/10/2008

A survey of the structural types known in zero-dimensional phosphonates revealed that the D4R (double-four-ring) core is quite common among main group phosphonates containing diamagnetic species such as Al(III), B(III), Ga(III), and Ti-(IV).[7a,12] In contrast, among analogous transition metal compounds, only two examples that possess a D4R core are known. One of them is a Co(II) phosphonate, $[Co_4(Ph_3CPO_3)_4Py_4]$ (Py = pyridine), which was reported by Winpenny et.al.,[8b] while the other is a Zn(II) phosphonate, $[t\text{-}BuPO_3Zn(2\text{-}APy)]_4$ (2-APy = 2-aminopyridine), reported by Murugavel and co-workers.[9f] Our experience in Cu(II) complex chemistry[8a,9a−d] has prompted us to search for this elusive example among copper(II) phosphonates. Previously we were able to assemble dodecanuclear[9a] and decanuclear[9c] copper phosphonates using the combination of *tert*-butylphosphonic acid and 3,5-dimethylpyrazole or 2-pyridylpyrazole. We wished to probe if the nuclearity of the aggregate can be reduced by using a pyrazole ligand containing sterically hindered substituents. Accordingly, in this paper we report the successful assembly, structural characterization, and magnetic properties of the first copper(II) phosphonate cage that possesses a D4R core. In addition, we have carried out studies relating to the nuclease activity of **1**. In recent years, there have been efforts to study the synergistic effect of multiple metal ion centers in conferring optimal nuclease activity.[13a] Recent observations by Guo and co-workers[13b] also suggest that the oxidative nuclease activity of multinuclear copper complexes can be manipulated by the geometry of the complex and by enhancing the number of metal centers. To the best of our knowledge, this is the first instance where a tetranuclear copper(II) aggregate has been shown to function as a plasmid modifier.

Table 1. Crystallographic Data and Structure Refinement Details of **1**

empirical formula	$C_{60}H_{116}N_8O_{12}Cu_4P_4$
formula weight	1519.65
temperature(K)	100(2) K
wavelength($Mo_{k\alpha}$)	0.710 73 Å
crystal system	monoclinic
space group	*C*2/*c*
unit cell dimensions	$a = 28.432(6)$ Å $b = 10.677(2)$ Å $c = 28.288(6)$Å $\beta = 119.39(3)°$
volume	7482(3) Å^3
Z, density (calcd)	4, 1.349 mg/m^3
absorption coefficient	1.265 mm^{-1}
F(000)	3216
crystal size (mm)	0.2 × 0.1 × 0.1 mm^3
θ range for data collection	2.08°−28.36°
limiting indices	$-26 \le h \le 37$, $-14 \le k \le 13$, $-37 \le l \le 32$
reflections collected/unique	24545/9224 [R(int) = 0.0824]
completeness to θ	98.5% (θ = 28.36°)
data/restraints/parameters	9224/0/423
goodness of fit on F^2	1.029
final R indices [$I > 2\sigma(I)$]	R1 = 0.0676, wR2 = 0.1382
R indices (all data)	R1 = 0.1030, wR2 = 0.1514
largest diff peak and hole	0.960 and −0.833 e Å^{-3}
refinement method	full-matrix least-squares on F^2

Experimental Section

Materials and General Methods. Solvents and other general reagents used in this work were purified according to standard procedures.[14a] $Cu_2(O_2CMe)_4{\cdot}2H_2O$ (Fluka) was used as obtained. *tert*-Butylphosphonic acid ($t\text{-}BuPO_3H_2$)[14b] and 3,5-di-*tert*-butylpyrazole ($3,5\text{-}t\text{-}Bu_2PzH$)[14c] were prepared according to published procedures. Supercoiled plasmid DNA (pBR322) was purchased from Bangalore Genei. Ethidium bromide was purchased from Sigma Aldrich Ltd. Magnesium monoperoxyphthalate hexahydrate (MMPP), procured from Lancaster, and sodium cacodylate buffer (SRL, Mumbai, India) were used as supplied. Ethylenediaminetetraacetic acid (EDTA), DMSO, *tert*-butyl alcohol, and D-mannitol were purchased from S. D. Fine Chemicals (Mumbai, India). All buffer solutions were prepared using Millipore water. IR spectra were recorded as KBr pellets on a Bruker Vector 22 FT IR spectrophotometer operating from 400 to 4000 cm^{-1}. Electronic spectra were recorded on a Perkin-Elmer-Lambda 20 UV−vis spectrometer and on a Shimadzu UV-160 spectrometer using dichloromethane as the solvent. Thermal gravimetric analysis and differential scanning calorimetry were carried out on a Perkin-Elmer, Pyris 6 thermogravimetric analyzer. ESI-MS spectra were recorded on a MICROMASS QUATTRO II triple quadrupole mass spectrometer. The ionization mechanism used was electrospray in positive ion full scan mode using methanol as solvent and nitrogen gas for desolvation. Capillary voltage was maintained at 3 kV and cone voltage was kept at 30 V. Magnetic susceptibility measurements were obtained with the use of a Quantum Design SQUID magnetometer MPMS-XL. This magnetometer works between 1.8 and 400 K for dc applied fields ranging from −7 to 7 T. Measurements were performed on finely ground crystalline samples of 41.28 mg. M vs H measurements were performed at 100 K to check for the presence of ferromagnetic impurities, which were found to be absent. The magnetic data were corrected for the sample holder and the diamagnetic contribution.

(9) (a) Chandrasekhar, V.; Kingsley, S. *Angew. Chem., Int. Ed.* **2000**, *39*, 2320. (b) Chandrasekhar, V.; Kingsley, S.; Vij, A.; Lam, K. C.; Rheingold, A. L. *Inorg. Chem.* **2000**, *39*, 3238. (c) Chandrasekhar, V.; Nagarajan, L.; Gopal, K.; Baskar, V.; Kögerler, P. *Dalton Trans.* **2005**, 3143. (d) Kingsley, S.; Chandrasekhar, V.; Incarvito, C. D.; Lam, M. K.; Rheingold, A. L. *Inorg. Chem.* **2001**, *40*, 5890. (e) Wu, J.; Song, Y.; Zhang, E.; Hou, H.; Fan, Y.; Zhu, Y. *Chem. Eur. J.* **2006**, *12*, 5823. (f) Murugavel, R.; Shanmugam, S. *Chem. Commun.* **2007**, 1257 references therein. (g) Yao, H-C.; Li, Y-Z.; Song, Y.; Ma, Y-S.; Zheng, L-M.; Xin, X-Q. *Inorg. Chem.* **2006**, *45*, 59. (h) Ma, Y-S.; Yao, H-C.; Hua, W-J.; Li, S-H.; Li, Y-Z.; Zheng, L-M. *Inorg. Chim. Acta* **2007**, *360*, 1645. (i) Yao, H.-C.; Wang, J.-J.; Ma, Y.-S.; Waldmann, O.; Du, W.-X.; Song, Y.; Li, Y.-Z.; Zheng, L.-M.; Decurtins, S.; Xin, X.-Q. *Chem. Commun.* **2006**, 1745. (j) Ma, Y-S; Song, Y; Li, Y-Z; Zheng, L-M. *Inorg. Chem.* **2006**, *45*, 5459 and references therein.

(10) Shanmugam, M.; Chastanet, G.; Mallah, T.; Sessoli, R.; Teat, S. J.; Timco, G. A.; Winpenny, R. E. P. *Chem. Eur. J.* **2006**, *12*, 8777.

(11) Comby, S.; Scopelliti, R.; Imbert, D.; Chabonnière, L.; Ziessel, R.; G. Bunzli, J.-C. *Inorg. Chem.* **2006**, *45*, 3158 references therein.

(12) (a) Diemert, K.; Englert, U.; Kuchen, W.; Sandt, F. *Angew. Chem. Int. Ed.* **1997**, *36*, 241. (b) Walawalkar, M. G.; Murugavel, R.; Roesky, H. W.; Schmidt, H.-G. *Inorg. Chem.* **1997**, *36*, 4202. (c) Walawalkar, M. G.; Murugavel, R.; Roesky, H. W.; Scmidt, H.-G. *Organometallics* **1997**, *16*, 516. (d) Yang, Y.; Walawalkar, M. G.; Pinkas, J.; Roesky, H. W.; Schimidt, H.-G. *Angew. Chem. Int. Ed.* **1998**, *37*, 96. (e) Mehring, M.; Guerrero, G.; Dalhan, F.; Mutin, P. H.; Vioux, A. *Inorg. Chem.* **2000**, *39*, 3325. (f) Mason, M. R.; Perkins, A. M.; Panomarova, V. V.; Vij, A. *Organometallics* **2001**, *20*, 4833.

(13) (a) Liu, C.; Wang, M.; Zhang, T.; Sun, H. *Coord. Chem. Rev.* **2004**, *248*, 147. (b) Zhao, Y.; Zhu, J.; He, W.; Yang, Z.; Zhu, Y.; Li, Y.; Zhang, J.; Guo, Z. *Chem. Eur. J.* **2006**, *12*, 6621.

(14) (a) Furniss, B. S.; Hannaford, A. J.; Smith, P. W. G.; Tatchell, A. R *Vogel's Text Book of Practical Organic Chemistry*, 5th ed.; ELBS and Longman: London, 1989. (b) Crofts, P. C.; Kosolapoff, G. M. *J. Am. Chem. Soc.* **1953**, *75*, 3379. (c) Yang, G.; Raptis, R. G. *Inorg. Chim. Acta* **2003**, *352*, 98.

Table 2. Selected Bond Lengths (Å) and Angles (deg) of **1**

bond distances (Å)		bond angles (deg)	
Cu−O and Cu−N	P−O and N−N (Å)		
Cu1−O1, 1.928(3)	P1−O3, 1.517(3)	O1−Cu1−N1, 160.89(15)	O3−P1−O4, 112.29(18)
Cu1−O4, 2.010(3)	P1−O4, 1.550(3)	O1−Cu1−O4, 86.41(13)	O3−P1−O5, 114.59(18)
Cu1−O5, 2.512(4)	P1−O5, 1.536(3)	O1−Cu1−O5, 105.05(12)	O5−P1−O4, 105.49(19)
Cu1−O6, 1.922(3)	P2−O1, 1.522(3)	O1−Cu1−O6, 95.38(14)	O1−P2−O2, 105.93(18)
Cu1−N1, 1.991(4)	P2−O2, 1.554(3)	O4−Cu1−O5, 64.70(12)	O6*−P2−O1, 115.55(18)
Cu2−O1, 2.604(3)	P2−O6*, 1.554(3)	O4−Cu1−O6, 163.31(15)	O6*−P2−O2, 111.81(18)
Cu2−O2, 2.013(3)	N1−N2, 1.363(5)	O4−Cu1−N1, 93.83(15)	P2−O1−Cu1, 143.4(2)
Cu2−O3, 1.928(3)	N3−N4, 1.363(5)	O5−Cu1−O6, 98.93(13)	P2−O2−Cu2, 103.62(16)
Cu2−O5*, 1.907(3)	N1−C5, 1.328(6)	O5−Cu1−N1, 92.23(15)	P1−O3−Cu2, 121.0(2)
Cu2−N4, 1.985(4)	N2−C7, 1.347(6)	O6−Cu1−N1, 89.86(15)	P1−O4−Cu1, 102.02(16)
	N3−C20, 1.339(6)	N2−N1−Cu1, 117.7(3)	P1−O5−Cu2*, 145.4(2)
	N4−C22, 1.340(6)	O1−Cu2−O2, 62.72(12)	P2*−O6−Cu1, 122.1(2)
	H31···O2*, 1.862(7)	O1−Cu2−O3, 98.92(12)	P1−O5−Cu1, 83.11(14)
	H32···O2*, 1.964(4)	O1−Cu2−N4, 91.48(15)	P2−O1−Cu2, 81.59(14)
		O1−Cu2−O5*, 103.13(13)	C5−N1−N2, 106.4(4)
		O2−Cu2−O3, 161.55(13)	C7−N2−N1, 111.7(4)
		O2−Cu2−O5*, 86.99(15)	C20−N3−N4, 112.1(4)
		O2−Cu2−N4, 92.76(16)	C2−N4−N3, 106.1(4)
		O3−Cu2−N4, 89.44(15)	
		O3−Cu2−O5*, 96.07(15)	N2−H31···O2*, 158.54(5)
		O5*−Cu2−N4, 163.33(15)	N3−H32···O4, 162.46(4)
		N3−N4−Cu2, 115.5(3)	
		Cu1−O5−Cu2*, 116.50(17)	
		Cu1−O5−Cu2, 112.69(13)	

Synthesis of $[Cu_2(3,5\text{-}t\text{-}Bu_2PzH)_2(t\text{-}BuPO_3)_2]_2$ (1). $Cu_2(OAc)_4 \cdot 2H_2O$ (0.50 mmol, 0.10 g) was taken in CH_2Cl_2 (30 mL). To this a solution were added 3,5-*t*-Bu_2PzH (0.50 mmol, 0.09 g), *tert*-butylphosphonic acid (0.50 mmol, 0.07 g) and triethylamine (1.00 mmol, 0.10 g) in CH_2Cl_2 (20 mL), and the mixture was stirred at room temperature for 12 h. The resulting clear blue solution was filtered and dried. The blue solid that was obtained was recrystallized from CH_2Cl_2/*n*-hexane mixture (1:1) to afford light blue crystals of **1**. Yield: 90%. Anal. Calcd for $C_{60}H_{116}Cu_4N_8O_{12}P_4$ (1519.65) (**1**): C, 47.48; H, 7.71; N, 7.39. Found: C, 47.32; H, 7.57; N, 7.25. IR (KBr, cm^{-1}): 3176 (s), 3101 (s), 2965 (s), 2866 (s), 2371 (s), 1579 (s), 1471 (s), 1380 (m), 1365 (s), 1305 (s), 1235 (s), 1205 (s), 1122 (s), 1025 (s), 998 (s), 960 (s), 828 (s), 780 (s), 730 (s), 665 (s), 583 (s), 523 (s), 448 (s). UV−vis (nm): 741.5. ESI-MS: $[M + 1]^+$ 1520.5.

X-ray Crystallography. Single-crystal X-ray structural studies were performed on a CCD Bruker SMART APEX diffractometer equipped with an Oxford Instruments low-temperature attachment. Data were collected at 153(2) K using graphite-monochromated Mo Kα radiation (λ_α = 0.710 73 Å). No decomposition of the crystal occurred during data collection. Data collection, structure solution, and refinement were performed using SMART,[15a] SAINT[15a] and SHELXTL[15b] All calculations for data reduction were done using the Bruker SADABS[15a] program. All non-hydrogen atoms are anisotropically refined using a full-matrix least-squares procedure. All hydrogen atoms except the N−H of pyrazole were included in idealized positions, and a riding model was used. The N−H hydrogen atoms were located from the difference Fourier maps and refined isotropically. All the H-bonding interactions, mean plane analyses, and molecular drawings were obtained using the program Diamond (version 3.1d)[15c]. The crystal and refinement data are summarized in Table 1, and selected distances and angles are shown in Table 2. Crystallographic data (atom coordinates, thermal parameters, and full tables of bond lengths and angles) have been deposited with the Cambridge Crystallographic Data Center (CCDC No. 643441). Copies of this information can be obtained free of charge from CCDC [12 Union Road, Cambridge CB2 1EZ, UK. Fax: +44(1223) 336−033. E-mail: deposit@ccdc.cam.ac.uk. URL: http://www.ccdc.cam.ac.uk.].

(15) (a) Bruker Analytical X-ray Systems, Madison, WI, 2001. (b) SHELXTL-PC Package, Bruker Analytical X-ray Systems, Madison, WI, 1998. (c) DIAMOND version 3.1d, Crystal Impact GbR, Bonn, Germany, 2004.

pBR322 Cleavage Assay. Plasmid cleavage reactions were performed in sodium cacodylate buffer (10 mM, pH 7.5, 32 °C), containing pBR322 (8 ng/μL, Bangalore Genei), a solution of **1** (1 mM) in distilled methanol, and magnesium monoperoxyphthalate (MMPP, 100 μM). For each cleavage reaction, 16−18 μL of pBR322 supercoiled DNA and 2 μL of complex **1** were used, and the reaction was initiated by adding 2 μL of magnesium monoperoxyphthalate in an Eppendorf tube. For scavenger experiments, the concentrations used were 100 mM. All cleavage reactions were quenched with 5 μL of loading buffer containing 100 mM of EDTA and 50% glycerol in Tris−HCl (pH 8.0). After this, the samples were loaded onto 0.7% agarose gel (Biozym) containing ethidium bromide (1 μg/1 mL). Electrophoresis was done for 1 h at constant current (80 mA) in 0.5× TBE buffer. Gels were imaged with a PC-interfaced Bio-Rad Gel Documentation System 2000.

Plasmid Cleavage under Anaerobic Conditions. Oxygen-free nitrogen was bubbled through cacodylate buffer, which was then subjected to four freeze−thaw cycles. All reagents were transferred in an argon-filled glove bag and Eppendorf tubes were tightly sealed with Parafilm in the argon atmosphere. Reactions were quenched with loading buffer and efforts were made to ensure strict anaerobic conditions during irradiation and quenching.

Results and Discussion

Synthesis and Structure. The reaction of $Cu_2(O_2CMe)_4 \cdot 2H_2O$ with *tert*-butylphosphonic acid (*t*-$BuPO_3H_2$) and 3,5-di-*tert*-butylpyrazole (3,5-*t*-Bu_2PzH) in the presence of triethylamine in dichloromethane (DCM) afforded $[Cu_2(3,5\text{-}t\text{-}Bu_2PzH)_2(t\text{-}BuPO_3)_2]_2$ (**1**) as a light-blue solid in about 90% yield (Scheme 1). The ESI-MS spectrum of **1**, in the positive ion mode, in methanol showed a M + 1 peak at *m*/*e* 1520.5, indicating the retention of its tetrameric structure, which is found in the solid state (vide infra). The electronic spectrum

Scheme 1. (a) Synthesis of **1** and Harris Notation for the Coordination Modes of (b) $[t\text{-BuPO}_3]^{2-}$ and (c) (3,5-t-Bu_2PzH)

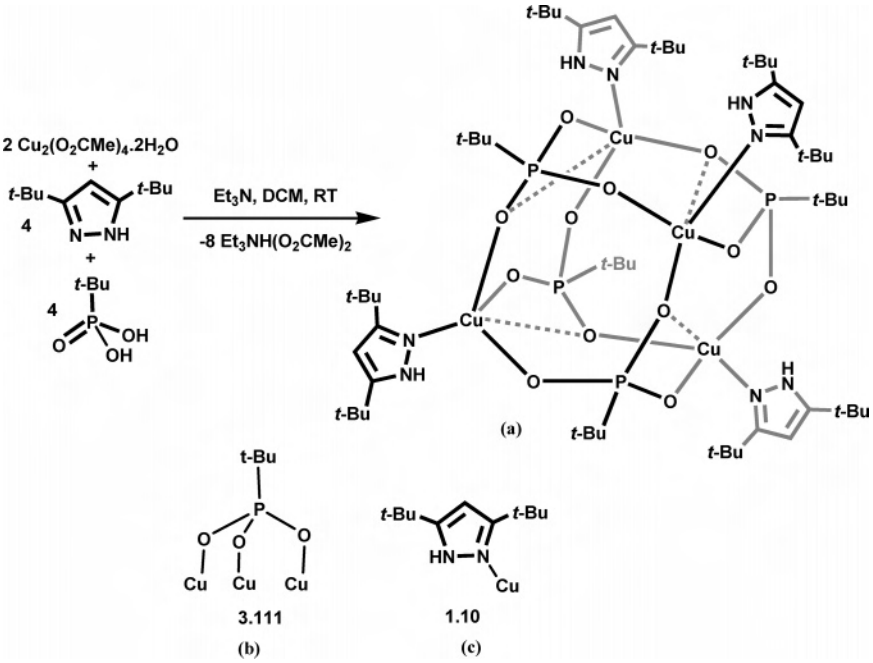

of **1** in CH_2Cl_2 displays a broad absorption at 741.5 nm (ϵ = 276 dm^3 mol^{-1} cm^{-1}).

Light-blue crystals of **1** suitable for X-ray diffraction were obtained from its solution of DCM/*n*-hexane. The molecular structure of **1** showed that it is a neutral tetranuclear copper(II) phosphonate cage in distorted cubic structure (Figures 1 and 2). Alternate corners of the distorted cube are occupied by copper and phosphorus atoms (Figure 2a). The top and bottom faces of the cubic core containing the $Cu_2P_2O_4$ unit represent two individual S4R (single-four-ring) cores that are connected through phosphonate bridges to form the D4R core (Figures 1 and 2b). This represents an unprecedented structural form for copper phosphonates. Although the cubic cage is not regular, it does possess a center of inversion.

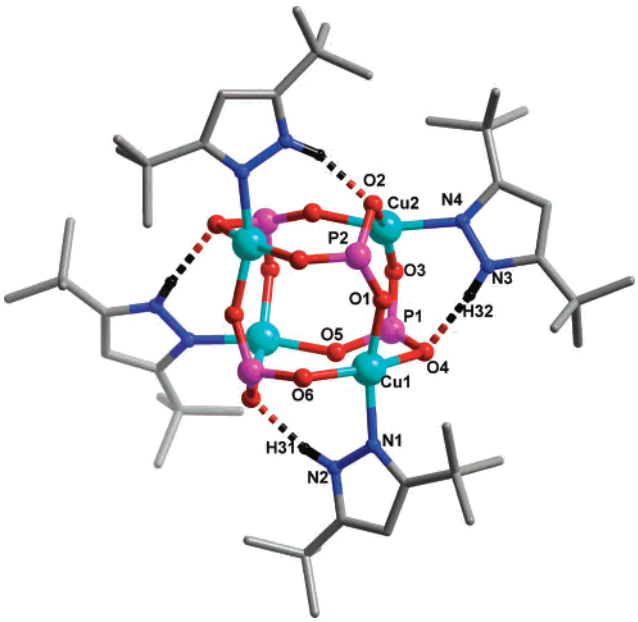

Figure 1. Molecular structure of **1**. The *tert*-butyl groups of phosphonic acid have been removed for clarity.

Each of the 12 edges of the cube contains a μ-O derived from the dianionic phosphonate ligand. As a result of this, the six faces of the distorted cubic core consist of puckered eight-membered $Cu_2P_2O_4$ rings (Figures 1 and 2b). Two types of eight-membered rings are present, four of one type (A) and two of another (B) (Figure 3). All four eight-membered rings of type A are contiguous and can be described as the top, bottom, and sides of the cubic core and have a similar half-chair conformation with one oxygen atom significantly deviating from the mean plane of the ring (Figures 2b and 3a). The rings of the type B can be described as the front and back of the cubic core and possess a twisted boat conformation. Within this, four atoms are in one plane and the other four atoms in another plane, the dihedral angle between these two planes being 46.5° (Figures 2b and 3b).

The multidentate phosphonate ligand holds the cage structure together. Each phosphonate ligand binds to three copper atoms in a 3.111 coordination mode (Scheme 1).[16] It is interesting to compare the binding mode of the phosphonate ligand in two other tetranuclear copper(II) phosphonates. In $[Cu_2(\mu\text{-Cl})(\mu_3\text{-MePO}_3)(Cl)(DMPZH)_3]_2$ (DMPZH = 3,5-dimethylpyrazole), the $[MePO_3]^{2-}$ ligand is tripodal.[9b] Two such ligands are involved in a bicapping coordination, holding a planar array of four copper atoms together in a 4.211 coordination mode.[16] On the other hand, in $[Cu_4(\mu_3\text{-OH})_2\{(ArP(O)_2(OH)\}_2(MeCO_2)_2(DMPZH)_4]^{2+}[MeCOO^-]_2\cdot CH_2Cl_2$ (Ar = 2,4,6-triisopropylphenyl) the $ArPO_3H_2$ functions as monoanionic ligand (3.210 mode of coordination to

(16) Harris notation describes the binding mode as $[X.Y_1Y_2Y_3...Y_n]$, where X is the overall number of metals bound by the whole ligand and each value of Y refers to the number of metal atoms attached to the different donar atoms. See: R. A. Coxall, S. G. Harris, D. K. Henderson, S. Parsons, P. A. Tasker and R. E. P. Winpenny, *J. Chem. Soc., Dalton Trans.*, **2000**, 2349.

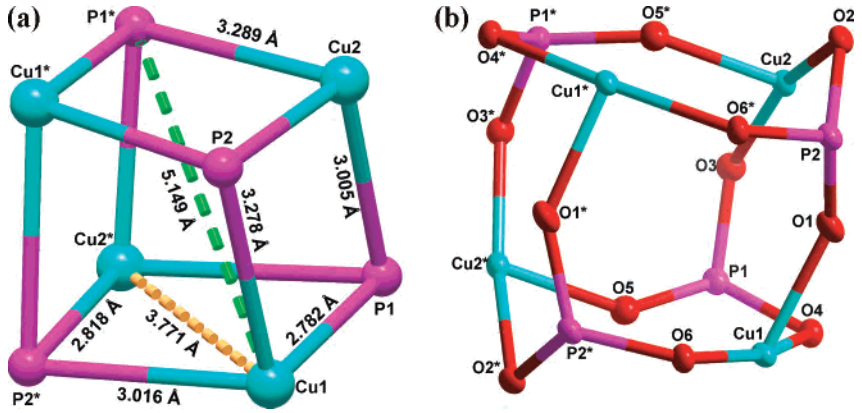

Figure 2. (a) Distorted cubane core of **1**. Edges and diagonal distances are given in the figure. Bond angles (deg): Cu1−P1−Cu2, 81.8(4); Cu1−P2−Cu2, 76.5(3); Cu1−P2*−Cu1*, 89.5(4); Cu1−P2*−Cu2*, 80.5(4); P2*−Cu2*−P1*, 103.8(4); P2*−Cu1*−P1*, 97.9(4); P2*−Cu1−P1, 105.3(5); P2*−Cu1−P2, 84.7(4). (b) D4R core of **1**. Four eight-membered rings of type A: Cu1*−O4*−P1*−O5*−Cu2−O2−P2−O6*; Cu2−O2−P2−O1−Cu1−O4−P1−O3; Cu1−O6−P2*−O2−Cu2*−O5−P1−O4; Cu2*−O3*−P1*−O4*−Cu1*−O1*−P2*−O2*. Two eight-membered rings of type B: Cu1*−O6*−P2−O1−Cu1−O6−P2*−O1*; Cu2*−O3*−P1*−O5*−Cu2−O3−P1−O5.

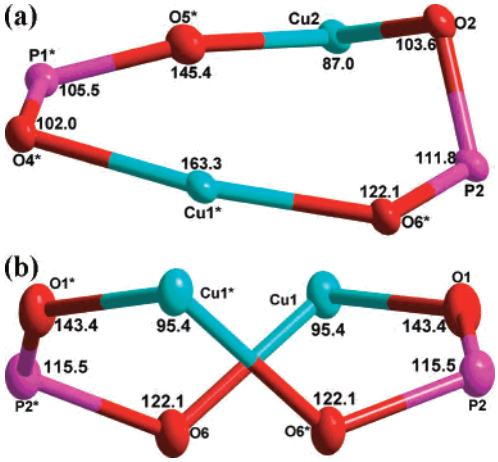

Figure 3. (a) Half-chair conformation of one of the type A rings. Bond angles at individual atoms are shown. O2 deviates from the mean plane of the ring by 0.99 Å (see Supporting Information). (b) Twisted-boat conformation of one of the type B rings.

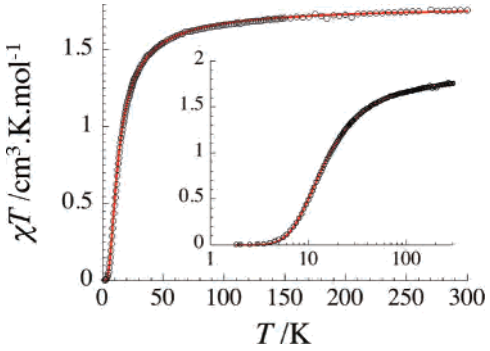

Figure 4. χT vs T plot for **1** obtained under 1000 Oe. The solid line shows the best fit of the experimental data to the model described in the text. Inset: χT vs T semilog plot.

copper atoms), and only two oxygen atoms are involved in coordination.[8a]

The 3,5-*t*-Bu_2PzH ligand in **1** is neutral and coordinates to the copper atom through its pyridinic nitrogen atom. There is a regular alternation of the arrangement of the 3,5-*t*-Bu_2-PzH ligand in terms of its coordinating nitrogen atom being in plane or perpendicular to the mean plane of the eight-membered ring that constitutes the face of the cubic core (Figure 1). This arrangement facilitates an intramolecular N−H···O hydrogen bonding between the *free* N−H of the 3,5-*t*-Bu_2PzH ligand and one of the phosphonate oxygen atoms (Figure 1). As a result of the coordination by the pyrazole ligand, each copper atom is tetracoordinate (3O, 1N) in a distorted square planar geometry. Among the three Cu−O bond distances, two are slightly shorter than the other [Cu2−O2, 2.013(3) Å; Cu2−O3, 1.928(3) Å; Cu2−O5, 1.907(3) Å]. The Cu−N distance [Cu2−N4, 1.985(4) Å] is normal (Table 2). Among the O−Cu−O bond angles found around copper, two are very narrow, while one is quite wide, reflecting the distortion in the cubic structure [O3−Cu2−O2, 161.55 (13)°; O3−Cu2−O5*, 96.07(15)°; O2−Cu2−O5*, 86.99(15)°]. The P−O distances are also not equal and a variation is found [P1−O3, 1.517 (3) Å; P1−O5, 1.536-(3) Å; P1−O4, 1.550(3) Å]. A similar variation of P−O bond distances was observed in the tetranuclear complex [Cu_2(μ-Cl)(μ_3-$MePO_3$)(Cl) $(DMPZH)_3]_2$.[9b] A closer observation of the Cu−O bond distances in **1** reveals that each copper atom of the tetranuclear cage has further long Cu−O contacts [Cu2−O1, 2.604(3) Å and Cu1−O5, 2.512(4) Å] (see Supporting Information).

Magnetism. Magnetic susceptibility measurements on a polycrystalline sample of **1** have been performed at 1000 Oe between 1.8 and 300 K. The data are presented as a χT vs T plot in Figure 4. At 300 K, the χT product amounts to 1.8 cm^3 K/mol, in agreement with the presence of four isolated $S = 1/2$ Cu(II) spins ($C = 1.81$ cm^3 K/mol with $g = 2.2$). When the temperature is lowered, the χT product continuously decreases to reach a value very close to zero at 1.8 K. This behavior is typical for the presence of dominant antiferromagnetic interactions between Cu(II) ions that leads to an $S = 0$ ground state.

According to the crystal structure symmetry, **1** possesses two types of Cu···Cu magnetic interaction (Scheme 2). The shortest Cu1···Cu2 and Cu1···Cu2* linkages involve two different μ-O bridges. From a magnetic point of view, the

Scheme 2. Spins and Magnetic Interactions Topology in **1**

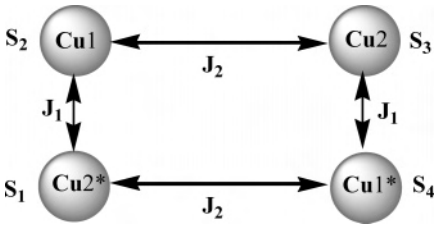

Cu1···Cu2* interaction (J_1) is the most significant one, because Cu−O bond distances are shorter (Cu1−O5, 2.513 Å and Cu2*−O5, 1.906 Å) and the Cu1−O5−Cu2* angle is larger (116.4°), favoring larger antiferromagnetic interactions than for the Cu1···Cu2 linkage (J_2) (Cu1−O1, 1.927 Å; Cu2−O1, 2.603 Å; Cu1−O1−Cu2, 112.8°). On the basis of this structural description (Scheme 2), the magnetic data were analyzed with the following Heisenberg spin Hamiltonian:

$$H = -2J_1\{S_1S_2 + S_3S_4\} - 2J_2\{S_2S_3 + S_4S_1\}$$

From this spin Hamiltonian, an analytical expression of the magnetic susceptibility has been given by Kolks and coworkers[17] in the $\mu_B H/k_B T \ll 1$ approximation:

$$A = J_1 + J_2 \quad \text{and} \quad F = 2(J_1^2 + J_2^2 - J_1J_2)^{1/2}$$

$$\chi = \frac{2Ng^2\mu_B^2}{k_B T} \left\{ \frac{5\exp(A/k_B T) + B}{5\exp(A/k_B T) + 3B + \exp((F-A)/k_B) + \exp(-(F+A)/k_B)} \right\}$$

with

$$B = \exp((J_1 - J_2)/k_B T) + \exp((J_2 - J_1)/k_B T) + \exp(-(J_1 + J_2)/k_B T)$$

A least-square fit using this susceptibility expression leads to the following set of parameters: $J_1/k_B = -10.6(2)$ K, $J_2/k_B = -3.3(3)$ K, and $g = 2.18(1)$, in excellent agreement with the experimental data, as seen in Figure 3. This set of parameters confirms the singlet ground state of **1**.

Nuclease Activity. Although many copper complexes have been examined as artificial nucleases, there are no reports on the use of multicopper aggregates (>3) for this purpose.[18] We were interested in examining if **1** could be used as a plasmid-cleavage reagent. Accordingly, we have systematically examined the DNA cleavage ability of **1**. Time course

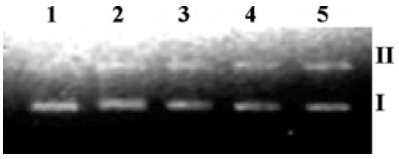

Figure 5. Complex **1**-mediated pBR322 DNA cleavage experiment at different time intervals: lane 1, DNA alone; lanes 2−5, DNA + complex 1 (30, 60, 90 and 120 min, respectively).

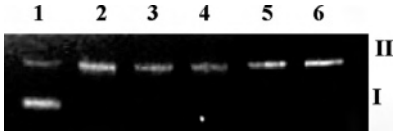

Figure 6. pBR322 DNA cleavage effected by complex **1** at different time intervals: lane 1, DNA alone; lanes 2−6, DNA + complex + MMPP (1, 2, 3, 4, and 5 min respectively). The data reveal that compound **1** is showing 100% (within 1 min) and 40% (120 min) conversion of DNA form I to nick form II, in the presence and absence of external oxidant MMPP, respectively.

experiments revealed that 40% conversion of the supercoiled pBR322 DNA form I to nick form II was achieved in 120 min in the presence of **1** (Figure 5). To foster the reaction, we have added magnesium monoperoxyphthalate (MMPP). In all such reactions, we observed a rapid conversion of the supercoiled pBR322 DNA form I to form II within 1 min (Figure 6). The nuclease activity of copper complexes occurs through oxidative[19] and/or hydrolytic[20] pathways, as described in recent literature. We probed the cleavage mechanism of **1** by performing the reactions in the presence of hydroxyl radical scavengers. Dimethyl sulfoxide (DMSO), D-mannitol, and *tert*-butyl alcohol did not inhibit cleavage reactions at all, clearly demonstrating the lack of direct involvement of such hydroxyl radicals (Figure 7). On the other hand, complete inhibition occurs in the presence of the singlet oxygen quencher, NaN_3. The crucial role of copper ions is also indicated by the inhibition of plasmid cleavage in the presence of EDTA. Interestingly, the DNA cleaving ability of **1** does not decrease under anaerobic conditions (Figure 8). This suggests that the Cu(II) species present in **1** interacts with MMPP, leading to the possible oxidative cleavage of DNA. A similar observation has been reported

(17) Kolks, G.; Lippard, S. J.; Waszczak, J. V.; Lilienthal, H. R. *J. Am. Chem. Soc.*, **1982**, *104*, 717.

(18) Selected references of trinuclear Cu(II) complexes showing DNA cleavage: (a) Humphreys, K. J.; Karlin, K. D.; Rokita, S. E. *J. Am. Chem. Soc.* **2001**, *123*, 5588. (b) Humphreys, K. J.; Karlin, K. D.; Rokita, S. E. *J. Am. Chem. Soc.* **2002**, *124*, 8055. (c) Korniyama, M.; Kina, S.; Matsumura, K.; Sumaoka, J.; Tobey, S.; Lynch, V. M.; Anslyn, E. *J. Am. Chem. Soc.* **2002**, *124*, 13731. (d) González-Álvarez;Alzuet, G.; Borrás, J.; Macias, B.; Castineras, A. *Inorg. Chem.* **2003**, *42*, 2992. (e) An, Y.; Liu, S-D.; Deng, S-Y.; Ji, L-N.; Mao, Z-W. *J. Inorg. Biochem.* **2006**, *100*, 1586. (f) Chen, J.; Wang, X.; Shao, Y.; Zhu, J.; Zhu, Y.; Li, Y.; Xu, Q.; Guo, Z. *Inorg. Chem.* **2007**, *46*, 3306 and references therein.

(19) Selected references for DNA cleavage involving oxidative pathway: (a) Sigman, D. S.; Bruce, T. W.; Sutton, C. L. *Acc. Chem. Res.* **1993**, *26*, 98. (b) Pogozelski, W. K.; Tullius, T. D. *Chem. Rev.* **1998**, *98*, 1089. (c) Burrows, C. J.; Muller, J. G. *Chem. Rev.* **1998**, *98*, 1109. (d) Bales, B. C.; Kodama, T.; Weledji, Y. N.; Pitié, M.; Meunier, B.; Greenberg, M. M. *Nucleic Acids Res.* **2005**, *33*, 5371. (e) Pitié, M.; Boldron, C.; Pratviel, G. *Adv. Inorg. Chem.* **2006**, *58*, 77.

(20) Selected references for DNA cleavage involving a hydrolytic pathway: (a) Hegg, E. L.; Burstyn, J. N. Coord. Chem. Rev. **1998**, *173*, 133. (b) Pope, L. M.; Reich, K. A.; Graham, D. R.; Sigman, D. S. *J. Biol. Chem.* **1982**, *257*, 12121. (c) Madhavaiah, C.; Verma, S. *Chem. Commun.* **2003**, *6*, 800. (d) Chandrasekhar, V.; Deria, P.; Krishnan, V.; Athimoolam, A.; Singh, S.; Madhavaiah, C.; Srivatsan, S. G.; Verma, S. *Bioorg. Med. Chem. Let.* **2004**, *14*, 1559. (e) Chandrasekhar, V.; Nagendran, S.; Azhakar, R.; Kumar, R. M.; Srinivasan, A.; Ray, K.; Chandrashekar, T. K.; Madhavaiah, C.; Verma, S.; Priyakumar, U. D.; Sastry, N. G. *J. Am. Chem. Soc.* **2005**, *127*, 2410. (f) Chandrasekhar, V.; Athimoolam, A.; Krishnan, V.; Azhakar, R.; Madhavaiah C.; Verma, S. *Eur. J. Inorg. Chem.* **2005**, *8*, 1482. (g) Sankar, J.; Rath, H.; Prabhuraja, V.; Gokulnath, S.; Chandrashekar, T. K.; Purohit, C. S.; Verma, S. *Chem. Eur. J.* **2006**, 13, 105 and references therein.

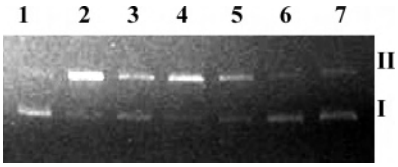

Figure 7. pBR322 DNA cleavage experiments in presence of free radical scavengers and singlet oxygen quencher assisted by complex **1** in a 2 min reaction: lane 1, DNA alone; lane 2, pBR322 + 1+ MMPP; lane 3, pBR322 + 1+ MMPP + DMSO; lane 4, pBR322 + 1 + MMPP + D-mannitol; lane 5, pBR322 + 1 + MMPP + *t*-BuOH; lane 6, pBR322 + 1 + MMPP + EDTA; lane 7, pBR322 + 1 + MMPP + NaN3. Conversion of form I to form II occurs even in the presence of reactive species like DMSO, D-mannitol, *t*-BuOH. Complete inhibition of DNA cleavage is noticed in the presence of NaN_3 and EDTA.

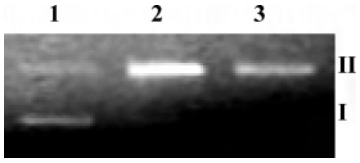

Figure 8. pBR322 DNA cleavage in anaerobic conditions experiment by complex **1** at different time intervals: lane 1, DNA alone; lanes 2−3, DNA + complex + MMPP. DNA cleaving reactivity of complex **1** does not decrease under anaerobic conditions.

earlier by other workers in the case of MMPP-assisted plasmid modification by Mn(II),[21a] Ni(II),[21b] or Cu(II)[21c] complexes.

Thermal Analysis. All the D4R main group metal cubic phosphonates $(MR)_4(R'PO_3)_4$ (M = B, Al, Ga, In; R′= *tert*-butyl) are thermally stable, and most of them were found to either melt or decompose after 280 °C.[7a,12] The thermoreversibility found from the DSC trace of **1** reveals that the tetranuclear core is stable up to the temperature of 280 °C (Figure S6). TGA analysis of **1** shows an initial weight loss of 40% at around 290 °C, which corresponds to the loss of four *t*-Bu_2Pz molecules, after which there is again a loss of about 20% at 400 °C, which corresponds to the loss of a P_4O_{10} molecule; there is no significant loss of weight after this temperature. About 28% (by weight) of residue remains until 900 °C. Recently, Murugavel and co-workers have reported a D4R Zn(II) phosphonate made of 2-aminopyridine and *t*-$BuPO_3H_2$, where a similar pattern of weight loss was observed.[9f]

Conclusion

In conclusion, we have prepared a novel lipophilic tetranuclear copper phosphonate, **1**, which possesses an unprecedented D4R core structure. The synthesis of this compound was accomplished in high-yield, utilizing a three-component protocol involving copper(II) acetate, *tert*-butylphosphonic acid, and 3,5-di-*tert*-butylpyrazole. The critical role of the ancillary ligand in controlling the nuclearity of the copper aggregates becomes evident, considering that the use of 3,5-dimethylpyrazole affords a dodecanuclear cage, while using 2-pyridylpyrazole leads to the formation of a decanuclear cage. The tetranuclear cage **1** exhibits a singlet ground state induced by Cu−Cu antiferromagnetic interactions. Interestingly, **1** is found to be an artificial nuclease in the presence of an external oxidant. We are currently investigating reaction pathways that can enable the selective isolation of high-nuclearity copper phosphonates.

Acknowledgment. We are thankful to DST, India for financial support including support for a CCD X-ray Diffractometer Facility at IIT-Kanpur and also for support under the special bioinorganic chemistry initiative. R.C. would like to thank the CNRS, the University of Bordeaux 1, and the Conseil Régional d'Aquitaine for financial support. L.N. thanks CSIR, India and S.G. thank IIT-Kanpur for research fellowship. V.C. is thankful to the Department of Science and Technology for a J. C. Bose fellowship. V.C. is a Lalith Kapoor Professor at the Indian Institute of Technology−Kanpur.

Supporting Information Available: Experimental details, additional schemes and figures (Figures S1−S6, Table S1), and crystal data and CIF file for **1**. This material is available free of charge via the Internet at http://pubs.acs.org.

IC701948G

(21) (a) Mandal, S. S.; Kumar, N. V.; Varshney, U.; Bhattacharya, S. *J. Inorg. Biochem.* **1996**, *63*, 265. (b) Liang, Q.; Ananias, D. C.; Long, E. C. *J. Am. Chem. Soc.* **1998**, *120*, 248. (c) Srivatsan, S. G.; Parvez, M.; Verma, S. *J. Inorg. Biochem.* **2003**, *97*, 340 and references therein.